I&EC research
Industrial & Engineering Chemistry Research

ARTICLE

pubs.acs.org/IECR

Analysis of Optimal Control Problems and Plant Debottlenecking for Urea Granulation Circuits

Ivana M. Cotabarren,* Diego Bertín, Juliana Piña, and Verónica Bucalá

Department of Chemical Engineering, PLAPIQUI, Universidad Nacional del Sur, CONICET Camino La Carrindanga Km. 7, (8000) Bahía Blanca, Argentina

ABSTRACT: The optimal control of a complete urea granulation circuit is studied in this work. The dynamic circuit operation is modeled by means of population, mass, and energy balances for the equipment of an industrial urea granulation flowsheet. The objective for the optimal control of the granulation circuit is to drive the process from a given steady-state (corresponding to the nominal capacity of a large-scale plant) to another one, by maximizing the throughput during the transient. To this aim, realistic operating constraints are taken into account and, based on an analysis of the active physical limitations, different optimal control variables are selected (i.e., urea melt flow rate, granulator discharge area, and granulator fluidization air temperature and mass flow rate). The results provide new promising operating points, which can be achieved by tracking the calculated optimal time-trajectories for the selected control variables, and give insights into the main plant bottlenecks.

1. INTRODUCTION

The granulation process is widely used in manufacturing particulate solid materials that require specific sizes, shapes, or properties. This complex process involves the growth of small particles (seeds) by agglomeration or coating. The wet or melt granulation is performed spraying a liquid binder onto particles as they are agitated; the particles' size enlargement evolves by deposition and solidification of liquid binder droplets on the seeds surface. Granulation is considered as one of the most significant advances in the fertilizer industry, providing products with higher resistance and lower tendency for caking and lump formation.[1] Particularly, and among all the nitrogen-based fertilizers, granular urea is the most used with a market in continuous expansion. Global urea capacity is forecast to grow by 51.3 Mt between 2009 and 2014, to reach 222 Mt in 2014.[2]

A typical flowsheet of a conventional urea plant based on the fluidized bed granulation technology is shown in Figure 1. The main unit is the granulator, where small urea particles known as seeds (generally product out of specification) grow by deposition of a concentrated fertilizer solution followed by evaporation of the droplets water content and urea solidification promoted by the fluidization air.[3] The granulation unit is divided into several chambers; in general, the first three are for particle growth while the last ones (two or three) are for decreasing the granule temperature. The solids that leave the size enlargement unit are further cooled in a fluidized bed and subsequently discharged into a conveyor that transfers them to double-deck screens, where they are classified into product, oversize, and undersize streams. The product is transported to storage facilities, while the oversize fraction is fed to crushers for size reduction. The crushed oversize particles are then combined with the undersize granules and returned to the granulator as seeds.[4]

In general, the material that leaves the granulation unit presents a relatively small fraction of particles in the commercial size range; therefore, high recycle ratios are common. The recycle feeds back to the granulator mass, energy, and a given solids particle size distribution (PSD), leading to frequent oscillating operations. In extreme cases, periodical oscillations can result in plant shutdowns or permanent variations in plant capacity and product quality.[5,6] Nowadays, the effect of the granulation circuit operating variables on its behavior is not yet well understood; for this reason many plants of urea granulation around the world are still operated by trial and error.

Even though there are publications in the field of dynamics and control of granulation circuits, none of the reported studies covers completely the scope of this work. Wildeboer,[7] Adetayo,[8] Adetayo et al.,[6] Balliu,[9] and Balliu and Cameron[1] studied the dynamics and stability of circuits based on drum wet granulators, by solving mass, energy, and population balances. In addition, different control strategies have been applied to wet granulation (i.e., drum, pan, or high shear wet granulation):

(a) For example, Zhang et al.[10] implemented a simple proportional−integral (PI) controller to control the recycle size distribution, which is related to the granule mean size and moisture content, by manipulating the water flow rate to the drum.
(b) Pottmann et al.[11] introduced Model Predictive Control (MPC) strategies to control the granules PSD and density by manipulation of the binder flow rate.
(c) Gatzke and Doyle III[12] extended the Pottmann et al.[11] study by the formulation of soft constraints and a prioritized control strategy to avoid unattainable set-points.
(d) Sanders et al.[13] compared the use of a proportional−integral−derivative (PID) controller with a MPC strategy, by using a granulator model validated against laboratory scale unit data. As the model did not include the complete circuit, the manipulated and control variables were only related with the high shear granulator operating conditions.

Received: January 7, 2011
Accepted: September 22, 2011
Revised: September 5, 2011
Published: September 22, 2011

dx.doi.org/10.1021/ie200043z | *Ind. Eng. Chem. Res.* 2011, 50, 11996–12010

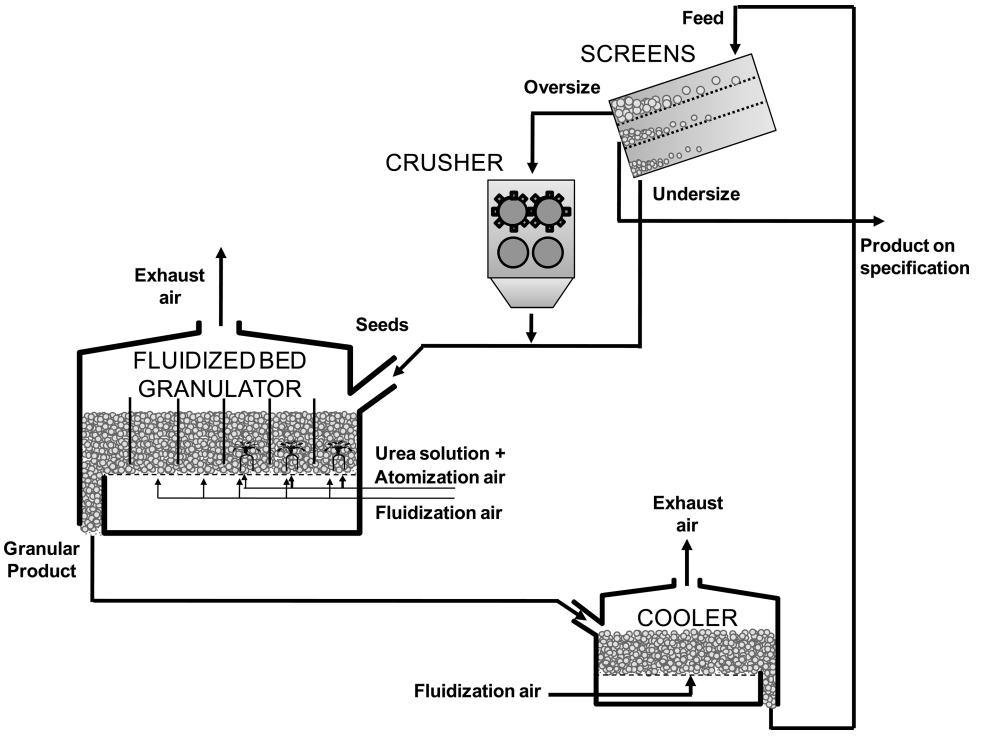

Figure 1. Typical urea granulation circuit.

(e) Finally, Glaser et al.[14] developed a robust MPC control strategy for a drum continuous granulation plant. They used models validated against experimental data from a pilot scale plant to analyze the process controllability with the aim of extending it to industrial scale. Glaser et al.[14] considered the fresh solid feed as manipulated variable for controlling the product PSD.

Regarding the optimization and optimal control of granulation systems, Wang et al.[15] applied (for different purposes) these techniques to batch and continuous wet drum granulation processes. Wang and Cameron[16] developed a multiform modeling approach to improve the applicability of the multilevel-model predictive control scheme (ML-MPC), resulting in effective strategies with significant reduction of computing time that allows their application in real time optimization (RTO) of drum granulation industrial plants. Summarizing, the previous results regarding optimization and optimal control studies have been mainly applied to wet granulation systems, where agglomeration plays an important role as growth phenomenon. Therefore, the aforementioned results cannot be straightforwardly extended to the fluidized bed melt granulation circuits where coating is the desired growth mechanism. Although, Heinrich et al.,[17] Heinrich et al.,[5] Drechsler et al.,[18] and Radichkov et al.[19] studied circuits including fluidized bed granulators, all these continuous units are constituted by just one chamber where wet granulation processes occur. In addition, either these authors assumed constant mass holdup for the granulator and/or hypothetical particle size distributions for the outlet crusher stream (i.e., the crusher operation is not modeled).

The previous facts together with the forecasted growth of the urea market constitute clear motivations to focus the research on urea granulation circuits to improve the efficiency of large-scale plants and increase their competitiveness. Complete mathematical models for all the circuit units have been developed in previous contributions, taking into account the particular characteristics of this system (i.e., melt granulation, granulator variable mass holdup, cooling stage, double-deck screens, and double-roll crushers). Cotabarren et al.[4,20] reported the urea double-roll crusher and double-deck vibrating screens models that were validated against industrial data from a large capacity plant. Bertín et al.[21] presented a novel model for the urea fluidized bed granulator which included dynamic mass, energy, momentum, and population balances. Based on these three models and one developed for the fluidized bed cooler,[22] the complete circuit simulator was implemented by Cotabarren et al.[22] The available simulation tool is very useful to explore new concepts of granulation circuits. In fact, it has been successfully used to perform steady-state optimizations by manipulating the crusher gap, screens apertures, and melt flow rate.[22] Therefore, based on a reliable simulator, the definition of efficient optimal control strategies for granulation circuits can be performed with confidence.

In this work, different optimal control studies are performed in order to maximize the plant throughput satisfying process physical limits as well as manipulated variables constraints. Four control variables are sequentially considered to maximize the plant capacity: urea melt flow rate, granulator discharge area, and granulator fluidization air mass flow rate and temperature. As a result, the main plant bottlenecks to meet the growing urea demand are identified and optimal time-trajectories for the manipulated variables are established.

2. MATHEMATICAL MODELS AND NUMERICAL TECHNIQUES

This section briefly describes the models developed for each of the units that constitute the granulation circuit under study; details of the model's formulation can be seen in the Appendix.

Regarding the size reduction stage, it is very common for urea production to use the double-roll type of crushers. These devices

are constituted by two pairs of rolls in series, which rotate in opposite directions at a certain speed. The rolls can be smooth or corrugated and the space or gap between them is variable, being a key parameter to adjust the PSD of the stream that leaves the device. The mathematical model to represent the urea granules fragmentation was presented in a previous contribution and it is summarized in the Appendix section.[4] This simulation tool, which is validated against experimental data from a high capacity granulation plant, allows determining the outlet crusher PSD as a function of the feed PSD and the gaps settings.

The classification step of the urea process is usually performed by double-deck vibrating screens. The screen mathematical model to classify the urea granules by size was reported by Cotabarren et al.[20] The authors fitted different model parameters to successfully predict oversize partition coefficients calculated from available plant data (model details are given in the Appendix).

For the multichamber fluidized bed granulator, the dynamic model developed by Bertín et al.[21] was used. This model is based on coating as the main size enlargement mechanism. To simulate the fluidized bed granulator, the nonsteady state mass, energy, momentum, and population balances were formulated and solved for all the granulator chambers (the granulator model is briefly presented in the Appendix). The fluidized bed cooler located downstream of the granulator operates as one of the granulator cooling chambers. Therefore, the cooler is represented by the mass and energy balance of any granulator chamber (reported in the Appendix) but setting the urea melt flow rate equal to zero.

During the operation of granulation circuits, a relatively low number of variables can be manipulated either continuously or periodically (among others, urea melt flow rate, gap between rolls in both pairs of the crusher, granulator and cooler fluidization air flow rate and inlet temperature, and granulator discharge area). In this work, different optimal control policies to maximize the plant capacity taking into account the limited number of possible manipulated variables and realistic system physical constraints are proposed.

Regarding the physical circuit constraints, there are some key limitations. The bed heights within each chamber cannot exceed the height of the chambers separating weirs to ensure that no solids overflow or bypass takes place. In addition, a minimum height is required to guarantee that the binder drops sprayed from the bottom nozzles are delivered within the bed. For these reasons, the bed heights were set to be within 50% and 88% of the weirs heights.

The temperatures in the growth chambers (first three) are restricted to a very tight range. They must be lower than the urea melting point (132 °C) to avoid partial or total bed quenching. Nevertheless, they need to remain higher than 100 °C to ensure a rapid evaporation of the urea solution water content. Therefore, the bed temperatures of the growth chambers have to lie between 100 and 120 °C.[23]

The product quality also constitutes an important system constraint; in fact, the product granulometry needs to be marketable. The granule quality is evaluated through different parameters, for example the mass fraction of product within the 2−4 mm size range ($W_{2-4\,mm}$) and the mass distribution median or Size Guide Number (SGN). The SGN represents the particle size in millimeters for which 50% by weight of the product is coarser and 50% is finer, multiplied by 100. According to the international standards, the granular urea SGN lies between 300 and 320.[24,25]

The gPROMS Model Builder Environment was chosen for the circuit model implementation. This is a multipurpose tool mainly used to build and validate process models, for steady-state and dynamic simulations and optimizations.[26] Its flexibility and robustness has been widely proved by many other workers who chose this environment for the dynamic optimizations of their process systems of different applications (Kiss et al., Lopez et al., Tzolakis et al., Asteasuain et al.).[27−30] Even for processes involving particulate solids (antisolvent crystallization by Nowee et al.[31]) gPROMS has proven to be an efficient environment for simulation and optimization.

In this work, the gPROMS tools provided for dynamic optimization were employed for the different optimal control problems. This environment offers two different standard mathematical solvers: the CVP_SS, which implements an algorithm based on single shooting, and the CVP_MS based on a multiple shooting algorithm.

In general, the CVP_MS is preferred when the model includes a large number of control variables and/or control intervals and few differential variables. CVP_SS is more suitable for big volume problems (large number of differential variables) with few decision variables (in comparison to the high number of differential equations). For the granulation circuit problem, there are about 270 differential equations and very few decision variables. Therefore, the CVP_SS is the solver selected in this contribution.

Besides the objective function, the manipulated variables, and the control intervals, gPROMS allows defining several types of model constraints: the end point constraints (which must be satisfied at the end of the operation), the interior point constraints (that hold at the extremes of the control intervals), and the path constraints (which must be satisfied at the entire operating time). The path constraints cannot be straightforward implemented, they require user programming. The way of enforcing the constraint (w) during the whole time horizon is to define a violation variable z through eq 1, and impose the end-point constraint $z(t_f) = \varepsilon$, with ε being a minimum tolerance.

$$\frac{dz}{dt} = (\max(0, w^{min} - w, w - w^{max}))^2 \quad z(0) = 0 \tag{1}$$

Thus, z will take the value of whatever is bigger, zero or the difference between the value of constraint w and its limits w_{min} and w_{max}. Therefore, the path constraints are solved as differential equations.[26]

CVP_SS can solve steady-state and dynamic optimization problems, with both continuous and discrete optimization decision variables. The solver to be used for integration of the model equations and their sensitivity equations, at each iteration of the optimization, can be either the standard DASOLV solver or a third-party differential-algebraic equation solver. In this contribution, the default DASOLV is used which is based on variable time step/variable order Backward Differentiation Formulas (BDF). This has been proved to be efficient for a wide range of problems. For optimization problems that do not involve any discrete decision variables, like the one analyzed in this contribution, the standard NonLinear Programming (NLP) solver to be used is the SRQPD solver. This employs a Sequential Quadratic Programming (SQP) method for the solution of the optimization. In our case, all the solver's parameters (DASOLV and SRQPD) have been used with their default values.[26]

3. RESULTS AND DISCUSSION

The objective for the optimal control problems analyzed through this work (by means of proper selection of the manipulated control

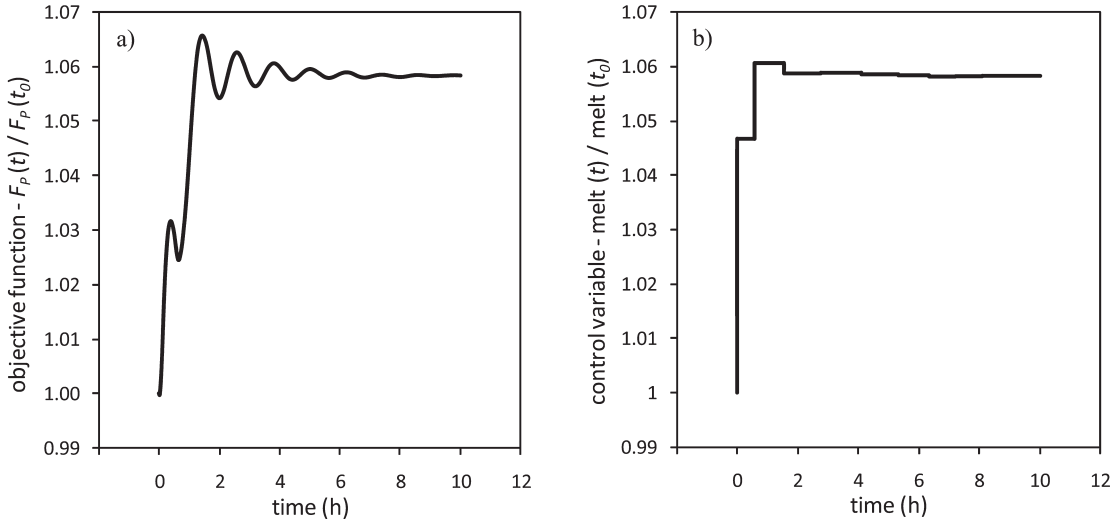

Figure 2. Throughput maximization by melt flow rate manipulation: (a) Objective function time-trajectory and (b) control variable-time trajectory.

variables time-trajectories) is to drive the process from an initial stable steady-state, corresponding to a large-scale plant operating at nominal capacity,[22] to another one by maximizing the throughput during the transient.

3.1. Maximum Product Flow Rate by Manipulating One Control Variable. The world-wide demand for urea dictates to the producing companies the need to increase, in a direct and feasible way, their throughput. The actual operation of granulation circuits does not allow significant changes in the production flow rate due to its complex effects on the system stability. Therefore, studies on this subject are specifically important in order to evaluate feasible plant revamps or establish the right dynamic profiles of the manipulated variables by satisfying the defined operating constraints.

As a first attempt, an optimal control problem for increasing the plant capacity by manipulating the total urea melt flow rate was performed. The total melt flow rate was equally distributed along three growth chambers. From Figure 1 it is clear that, if the dust generation in the granulator and cooler are neglected, the circuit becomes a system with one urea input (urea melt) and one urea output (granular product). Therefore, once a steady state is reached both flow rates should be equal. Consequently, the trivial solution to the above proposed optimal control problem would be to increase the urea melt as much as possible. However, due to the recycle and the many variables that affect the coupled mass, energy, and population balances of the granulator, many of the operating constraints are not necessary satisfied along the operating time. As a result, it becomes significant to determine the urea melt dynamic profile that ensures a feasible dynamic operation.

As it was aforementioned, different optimal control cases were implemented under the gPROMS environment. For this particular case of study, the following objective function was considered:

$$\mathrm{FO}(u(t)) = \max_{u(t),\, t\in[t_0,\, t_f]} \int_{t_0}^{t_f} F_P(x(t), u(t))\mathrm{d}t \qquad (2)$$

where $FO(u(t))$ represents the value of the objective function, $u(t)$ are the control variables (for this first case, $u(t)$ represents the urea melt flow rate profile), $F_P(t)$ is the urea production to be maximized from the initial to the final operating time, and $x(t)$ represents the state variables of the process model previously described and detailed in the Appendix. The optimal control problem was subjected to the following constraints:

$$300 \le \mathrm{SGN}_{\mathrm{product}}(t) \le 320 \qquad (3)$$

$$0.5H_{\mathrm{weir}} \le H_k(t) \le 0.88H_{\mathrm{weir}} \quad \text{for } k = 1 \text{ to } 6 \qquad (4)$$

$$100\ ^\circ C \le T_k(t) \le 120\ ^\circ C \quad \text{for } k = 1 \text{ to } 3 \qquad (5)$$

as well as to the constraints given by the circuit dynamic models stated on the Appendix.

The optimal control problem also requires the definition of the simulation final time as well as the number and duration of the control intervals. According to the disturbances imposed to the circuit in a previous work,[22] 10 h is a reasonable time for reaching a new steady state. The minimum duration of the control intervals was set in 10 min to ensure a feasible control in the industrial practice. Simulations for different number of control intervals indicated that a number of ten was the minimum one to achieve the optimal objective function value. It was also proved that time horizons smaller than 10 h but long enough to reach the new steady state, do not modify substantially either the control variables time-trajectories or the optimal objective function values. Besides, each of the optimizations was run several times using different initial time-trajectories ranging from the upper to the lower control variables limits. In all the cases the same value of the optimal objective function was found.

Figure 2a and b show the dynamic profile of the objective function (throughput) and the control variable (total melt flow rate, equally distributed between the growth chambers) for the proposed optimal control problem, respectively. Both variables are referred to their initial steady state values. The time-averaged product flow rate increases about 5.5%; this improvement is achieved by increasing the urea melt flow rate injected in the granulation chambers. Figure 3 presents the evolution over time of the selected circuit variables for this optimum trajectory. In this case, the chambers' heights (Figure 3a) are referred to the weir height. The bed height of the second growth chamber is the only variable that reaches the imposed constraint (Figure 3a) and this behavior is responsible for the achievement of a relatively low capacity improvement with respect to that of the initial operating

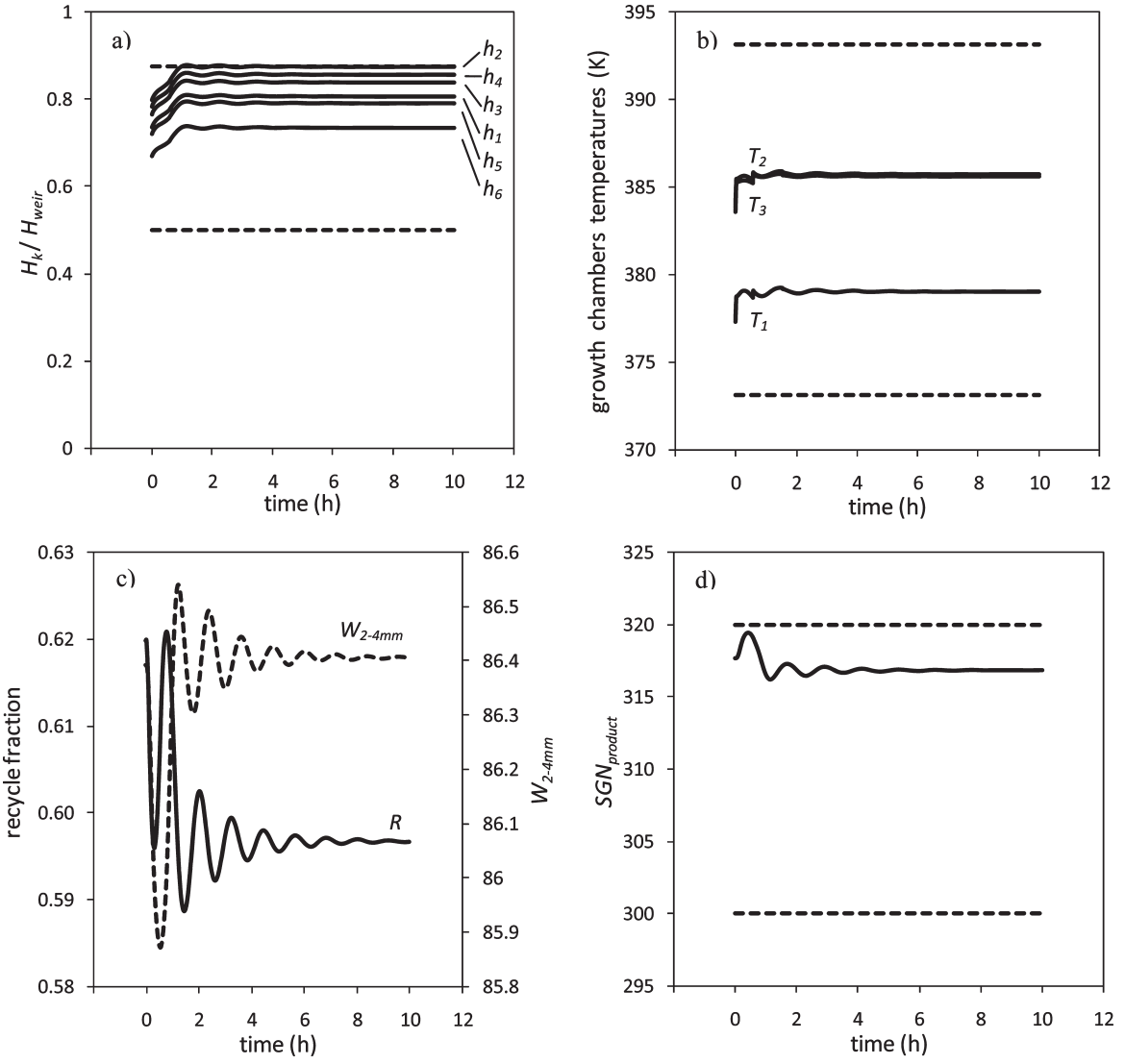

Figure 3. Throughput maximization by melt flow rate manipulation: selected circuit variables.

condition. Unsurprisingly, the higher the urea melt fed to each chamber, the higher the fluidized bed levels. The urea solution enters the granulator at a temperature around 130 °C, significantly higher than the growth chambers temperature. Therefore, the increment in the melt flow rate generates an extra energy contribution that increases the growth chambers temperatures as it can be seen in Figure 3b.

According to Figure 3c, the increment in the urea melt flow rate is accompanied by a decrease (−3.5% time-averaged) in the recycle fraction (R), which is defined as

$$R = \frac{F_O + F_U}{F_P} \tag{6}$$

F_O and F_U being the mass flow rate of the oversize and undersize (product out of specification) classified by the double-deck screens, respectively. Even though F_O and F_U increase as well as all the other circuit streams due to the higher melt mass flow rate (data not shown), the increments in F_P are more important leading to a lower R. The fraction of product on specification ($W_{2-4\ mm}$) presents a slight diminution at the initial time (−0.6%) but then tends to the value of the original steady state.

Regarding the effect of the melt mass flow rate on the circuit streams particle size, in Figure 3d it can be seen that the product SGN first increases and then decreases stabilizing on a smaller size than that corresponding to the initial steady state, within the defined constraints. Therefore, the throughput is increased preserving the product quality given by satisfactory SGN and $W_{2-4\ mm}$ values. It is worth mentioning that the first increment in the product SGN is limiting the urea melt injection for the first control interval. When the SGN starts to decrease due to the recycle influence on the granulator performance, the urea melt reaches its maximum value.

Assuming coating as the main particle enlargement mechanism, the net granule size growth in each granulator chamber is governed by the product between the growth rate (G_k) and the particle residence time (τ_k):

$$G_k \tau_k = \frac{2\dot{m}^k_{melt}(1 - x^k_{melt})}{\rho_p A p^k_T} \frac{m^k_T}{\dot{m}^k_{out}} \tag{7}$$

The growth rate (G_k) is a function of the urea melt mass flow rate fed to the granulator chamber k ($\dot{m}^k_{melt}$), the binder water

dx.doi.org/10.1021/ie200043z |*Ind. Eng. Chem. Res.* 2011, 50, 11996–12010

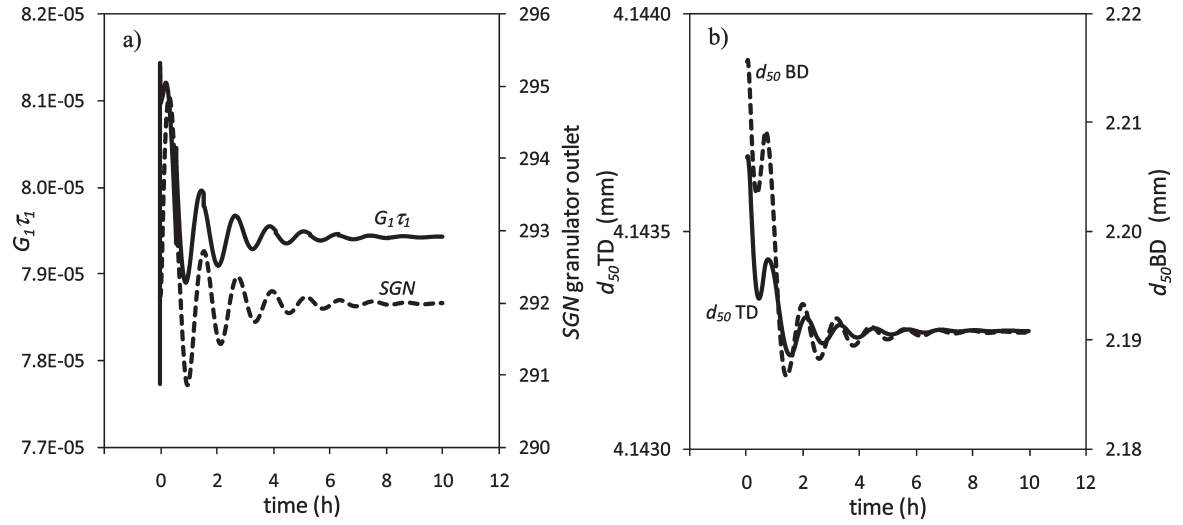

Figure 4. Throughput maximization by melt flow rate manipulation: (a) granulator growth analysis and (b) screens' cut sizes.

content (x^k_{melt}), the particle density (ρ_p), and the total particle superficial area within chamber k (Ap^k_T). According to eq 7, G_k states that all the particles, independently of their sizes, grow at the same rate.[21,32,33] The residence time depends on the solid mass holdup in granulator chamber k (m^k_T) and the particle mass flow rate coming out of the granulator chamber k ($\dot{m}^k_{out}$). As an example, Figure 4a shows for the first growth chamber the behavior of the product $G_1\tau_1$, together with the SGN corresponding to the stream leaving the granulation unit. It is verified that an increase in $G_1\tau_1$ produces bigger particles at the granulator outlet and vice versa. The granulator outlet SGN follows the $G_1\tau_1$ trend, slightly delayed by the granulator residence time. Even though the SGN at the granulator outlet stabilizes in a value nearly equal to the one corresponding to the initial steady state, the product SGN (Figure 3d) reaches a final value about 0.3% smaller than its corresponding initial steady state suggesting that another variable has an effect on the product SGN. In fact, the product stream is affected not only by the quality of the PSD at the granulator outlet but also by the screen performance. In this case, it is corroborated that the first increment in the product SGN is due to the bigger particles that reach the screen from the granulator. The global decrease with respect to the initial steady state, verified afterward, arises not only from the trend exhibited by the SGN at the granulator outlet but also from the diminution in the screens' cut size (d_{50}, i.e., the diameter at which each deck classifies the particles as oversize or undersize[20]). In fact, Figure 4b shows that both cut diameters (d_{50} TD for the top deck, and d_{50} BD for the bottom deck) decrease over time. A lower d_{50} (which is influenced by, among others, the screen feed quality and flow rate, and the deck characteristics) means that the mass median of the oversize stream (SGN) will shift toward smaller diameter.

Overall, this optimal control case points out that a capacity increment of about 5.5% is feasible, maintaining the desired product quality and also reducing the circuit recycle fraction. Nevertheless, the optimization is limited by the increment of the second chamber bed height, which reaches its maximum admissible value. To achieve higher throughputs, it is necessary to use a second control variable capable of regulating the bed heights. In this context, the granulator solids discharge area appears as an attractive variable to be manipulated. Actually, the granules are discharged from this unit by ducts located at the bottom of the last chamber. At the end of the ducts, a swing type valve is often used to control the solids discharge. The opening angle of this valve allows modifying the discharge area and thus to regulate the solids mass flow rate from the granulator.

3.2. Maximum Product Flow Rate by Manipulating Two Control Variables. Based on the above discussion, both the urea melt flow rate and granulator discharge area were established as control variables ($u(t)$) to be manipulated in order to maximize the objective function represented by eq 2, satisfying constraints 3, 4, and 5. To be consistent with the results of the first optimal control problem, the number of control intervals as well as their duration were kept at the same values (i.e., ten intervals, each of them at least 10 min long). For the initial steady state, the discharge area was 87% of the total available one. The mathematical equation that relates the solids flow rate at the granulator outlet with the discharge area can be found in the Appendix (A.12).[21] The discharge area was affected by a parameter α that represents the fraction of the actual discharge area with respect to the initial one. Therefore, α can vary from 0 (i.e., duct fully closed) to the maximum value of 1.15 (i.e., duct fully opened).

Figure 5a and b present the time evolution of the objective function and both manipulated variables respectively; all the variables are referred to their values at the initial steady state. The time-averaged value for the product flow rate is approximately 22% higher than the initial steady state throughput and significantly better than the one obtained by using just one control variable. Figure 5b indicates that the maximum capacity is achieved by increasing the urea melt flow rate (initially constrained by the product SGN upper limit) and by setting the discharge area at its maximum allowable value ($\alpha = 1.15$). The evolution of different important circuit variables can be appreciated in Figure 6. The chambers' heights (Figure 6a) present values lower than the initial steady state for the first half hour, while the discharge area increases up to its highest value allowing greater granulator discharge flow rates. Once the granulator discharge is fully opened, the bed levels increase until the second chamber height reaches the upper limit. Increments in the granulator discharge area allow higher urea melt flow rates into the chambers. As a result of this higher energy input, the increases in the growth chamber bed temperatures are more significant than in the previous optimization (Figure 6b). Concerning the recycle fraction and the fraction of

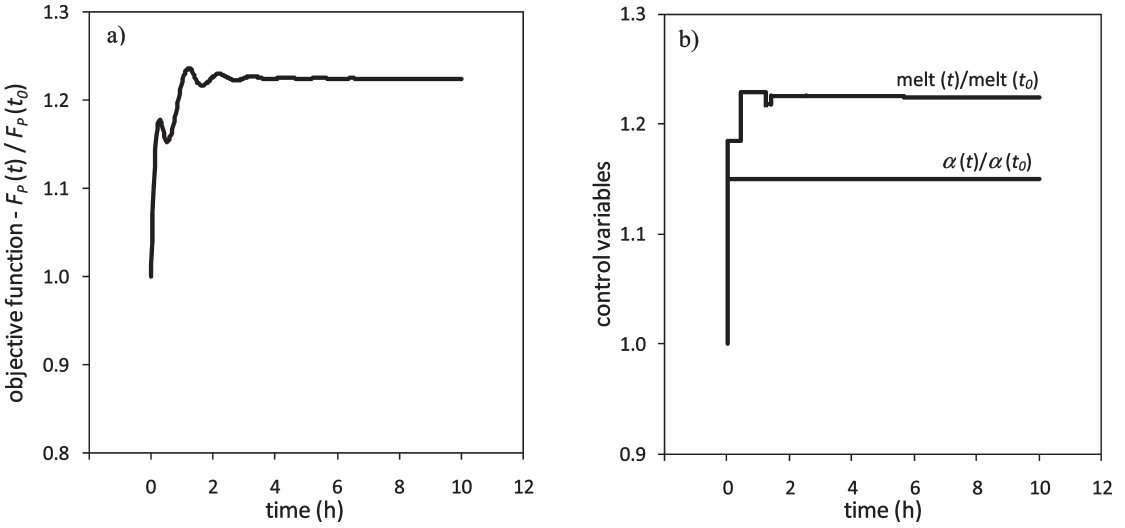

Figure 5. Throughput maximization by melt flow rate and solids discharge area manipulation: (a) objective function time-trajectory and (b) control variables time-trajectory.

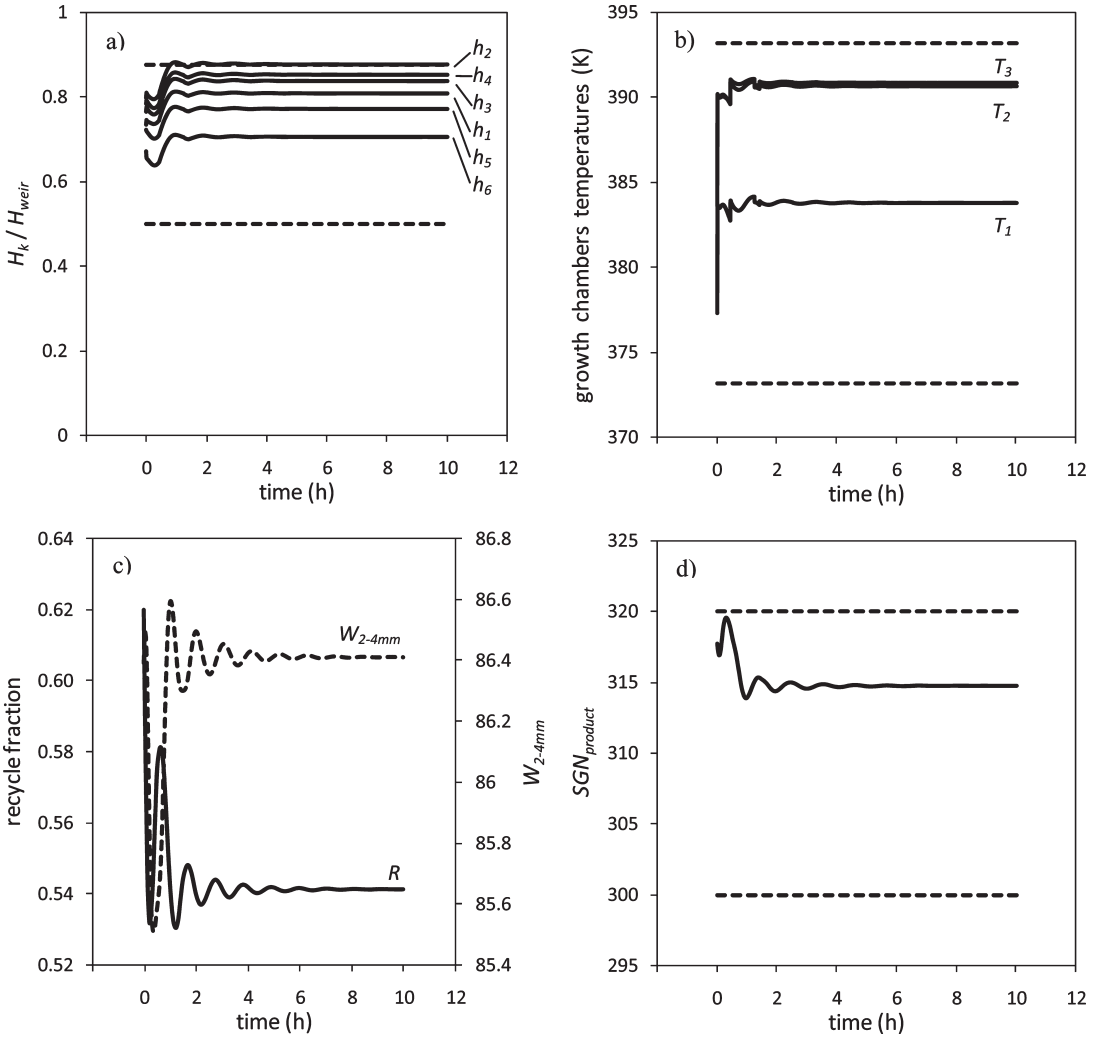

Figure 6. Throughput maximization by melt flow rate and solids discharge area manipulation: selected circuit variables.

product on specification (Figure 6c), a behavior similar to that presented in Figure 3c is observed. R decreases 12% with respect to its initial steady state value (basically because the throughput is considerably higher, see eq 5). The $W_{2-4\ mm}$ remains almost

dx.doi.org/10.1021/ie200043z |*Ind. Eng. Chem. Res.* 2011, 50, 11996–12010

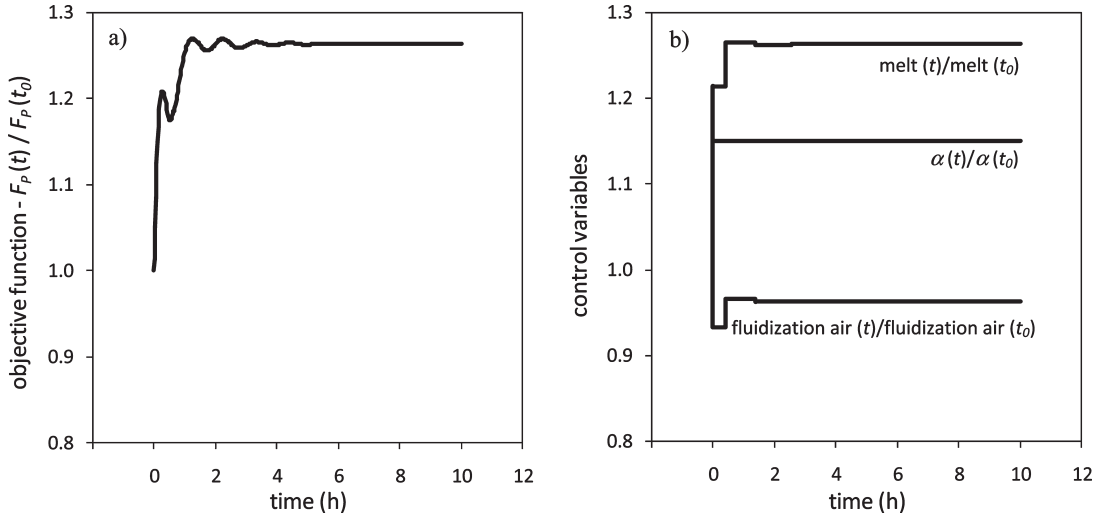

Figure 7. Throughput maximization by melt flow rate, solids discharge area, and fluidization air flow rate manipulation: (a) objective function time-trajectory and (b) control variable-time trajectory.

constant, except during a first period where it decreases about 1%. Once again, the product SGN (Figure 6d) initially increases following the same trend as the granulometry of the solids that leave the granulator (data not shown) and partially limiting the increment in the urea melt flow rate. Immediately afterward, it responds to the decrease in both the SGN at the granulator outlet and the screens d_{50} due to the significant changes in the screen feed flow rate.

This optimal control problem leads to a higher improvement in the objective function, but it is still restricted by the upper limit in the height of the granulator second chamber. Another variable that can be manipulated in the granulation circuit is the fluidization air flow rate that enters the granulator. In fact, the bed heights are directly affected by this variable; higher air flow rates (above the minimum fluidization condition) expand the bed to higher levels.[21] Therefore, a new optimal control case is introduced taking into account the fluidization air flow rate as the third control variable.

3.3. Maximum Product Flow Rate by Manipulating Three Control Variables. For this optimal control problem the objective function was described by eq 2 considering constraints 3, 4, and 5. The number and length of the control intervals was defined in the same way than for the previous cases.

As aforementioned, the new added control variable was the total fluidization air mass flow rate. The fluidization air flow rate was allowed to vary between 80 and 120% with respect to the base case. To define this range, the capacity of the available blower was considered. In addition, the operating limits imposed by the terminal velocity and the minimum fluidization velocity of the particles in the granulator were checked. The air flows fed to each chamber were calculated as a given fraction (corresponding to the ones defined for each chamber at the initial steady state) of the total air flow rate.

The evolution over time of the dimensionless objective function as well as the control variables for this optimization are shown in Figure 7. The product flow rate exhibits a time-average increment of about 26% with respect to its initial steady state value (3.7% more than the previous optimization). This increment is achieved by increasing the urea melt flow rate, setting the maximum allowable discharge area, and initially decreasing the total fluidization air flow rate.

Regarding the main variables behavior, Figure 8 shows the time evolution of the significant ones. Once again, the chamber heights are referred to the weir height. At the beginning, the chamber heights (Figure 8a) decrease due to the opening of the discharge area, then their upper limit is reached. Nonetheless, the temperature in the third growth chamber becomes immediately an active constraint. To decrease the bed heights, the fluidization air flow rate diminishes immediately. As a result, the cooling capacity decreases with a consequent increase in the chamber temperatures.

Both, the recycle fraction and the mass fraction of product on specification exhibit the same behaviors as those observed for the previous performed optimal control problems (Figure 8c). The time-averaged recycle ratio diminishes about 14% with respect to the initial R value and the $W_{2-4\ mm}$ remains almost unchanged. The product SGN (Figure 8d) increases at the beginning due to the growth of the particles coming out from the granulator, limiting the melt increment in the first control interval. Then, the product SGN decreases because not only the SGN at the granulator outlet but also both screens d_{50} are lower.

Once again, it is expected that the addition of an extra control variable (besides the three last tested) may improve the objective function as a consequence of more degrees of freedom. According to the results of the third case, the limiting active constraint is the temperature in the growth chambers. For this reason, the fluidization air temperature is contemplated as the fourth control variable.

3.4. Maximum Product Flow Rate by Manipulating Four Control Variables. This last optimal control problem was performed for the objective function as formulated in eq 2. The same constraints (eqs 3−5) and number and minimum duration of control intervals were applied. For this particular case, the temperature of the fluidization air entering the second chamber (Ta_2) was chosen as the new control variable. If this chamber is guaranteed to be cool enough, the third chamber will be as well since it is fed with the material coming out from the second chamber. The first chamber is generally cooler than the second one because it receives the recycle stream which is at a much lower temperature than the first bed. The fluidization air temperature was restricted to a minimum feasible value of 288 K, with 311 K being the initial steady state value.

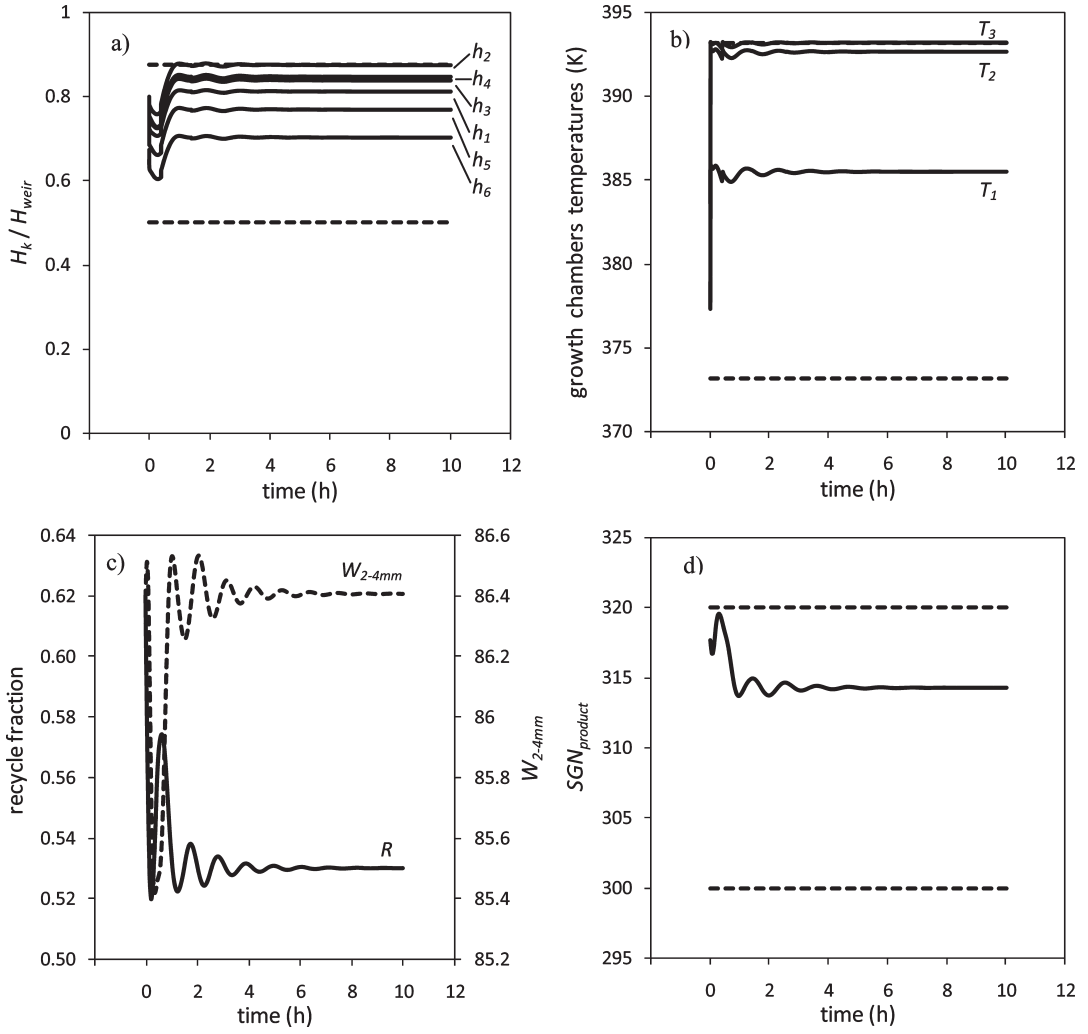

Figure 8. Throughput maximization by melt flow rate, solids discharge area, and fluidization air flow rate manipulation: selected circuit variables.

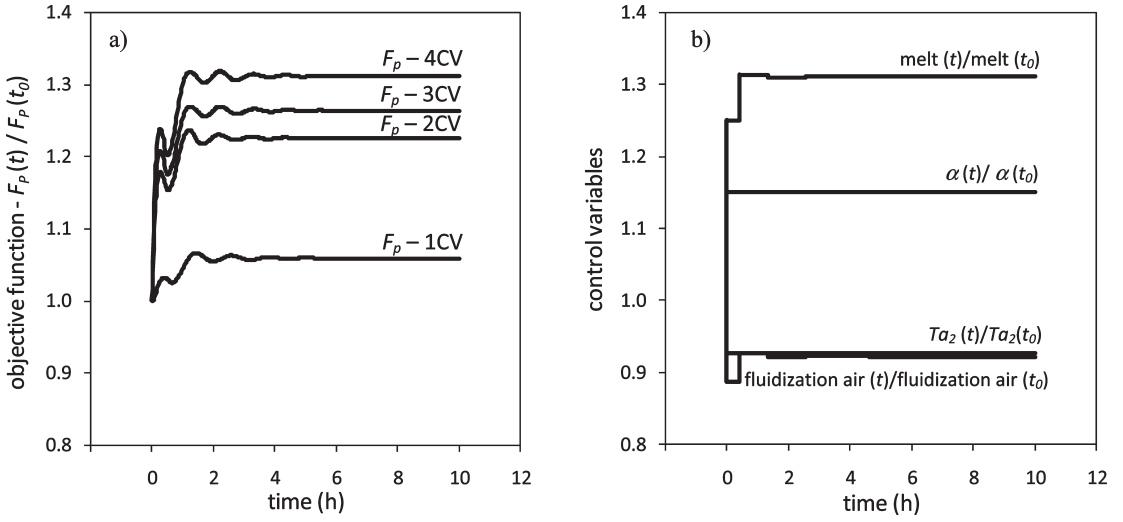

Figure 9. Throughput maximization by manipulation of the melt flow rate, solids discharge area, fluidization air flow rate, and inlet air temperature in the second chamber: (a) objective function time-trajectories and (b) control variables-time trajectories.

Figure 9a presents the evolution over time of the objective function obtained with four control variables. Together with this, the results of the other performed control problems are included in Figure 9a in order to clearly compare the benefits of adding

dx.doi.org/10.1021/ie200043z |*Ind. Eng. Chem. Res.* 2011, 50, 11996–12010

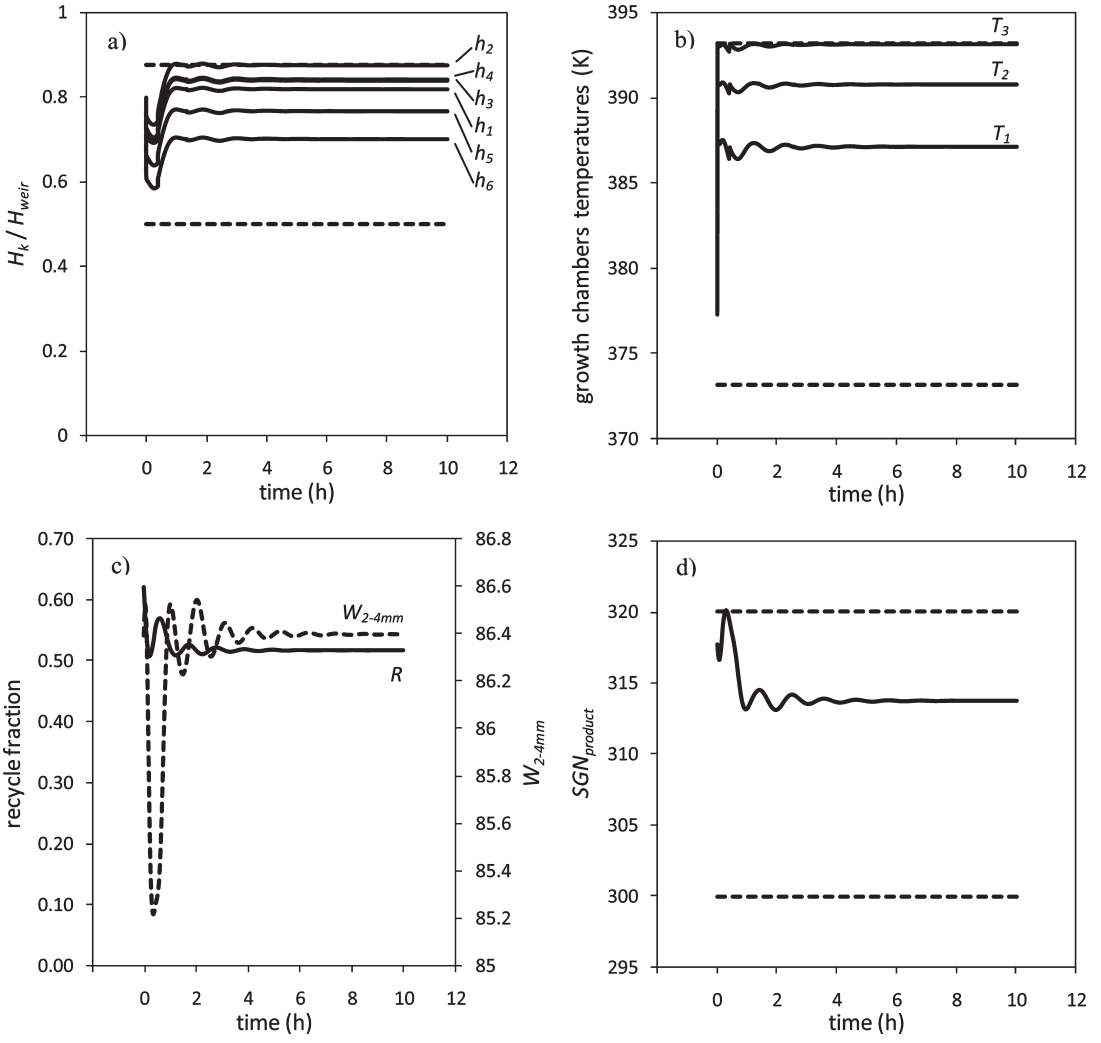

Figure 10. Throughput maximization by manipulation of the melt flow rate, solids discharge area, fluidization air flow rate, and inlet air temperature in the second chamber: selected circuit variables.

control variables. This last optimal control problem increases the time-averaged product flow rate in about 30% with respect to the initial steady state, against increments of 26% with three control variables, 22% with two, and 5.5% with just one manipulated variable. The dynamic profile of the four control variables is shown in Figure 9b. The capacity increment (due to the possibility of processing higher total urea melt flow rate) is achieved by setting the aperture of the discharge area at its maximum value, decreasing the fluidization air flow rate, and fixing the inlet temperature of the fluidization air to the second chamber at its lowest allowable level (288 K).

Regarding the circuit variables, behaviors similar to those described above are observed. Once again, the temperature in the third chamber is the limiting variable. Nonetheless, a significant decrease in the second chamber temperature is achieved through the cooling of the fluidization air (Figure 10b). The chamber levels decrease at the beginning due to the opening of the discharge area and then increase because of the higher mass holdup (Figure 10a). The recycle fraction decreases and the product mass fraction on specification remains constant, except once more for an initial decrease of around 1.2% (Figure 10c). In this particular case, the product SGN upper limit becomes an active constraint due to the important increment in the granulator net growth (Figure 10d).

It is worth mentioning that, according to the presented results, all the optimizations led to stable new steady states. Regarding the computing time invested during the performed optimization studies, for an Intel Core 2Duo 2GB processor it took approximately 50 min to solve the simplest case (i.e., one control variable) and 6 h and 30 min to find the solution for the more complex case analyzed (i.e., four control variables). This is in accordance with the magnitude of the problem: 9400 algebraic equations and 270 differential equations. Besides, the optimizations were performed for a large time horizon together with several constraints formulations (end point, interior point, and path constraints for all the cases).

3.5. Optimal Control under Model Uncertainties. The aim of this section is to evaluate the sensitivity of the previous optimization results to different model uncertainties. It is important to prove that similar conclusions are obtained in order to guarantee that the optimal profiles are practically applicable. For granulation processes, the need of taking into account the model uncertainties to evaluate optimal trajectories was first introduced by Wang and Cameron in different contributions.[16,35,36]

As a first step, the main model uncertainties were identified. In the granulation circuit described in this contribution, the models fitting parameters represent a source of uncertainties that are worth analyzing. According to the models presented in the Appendix, each of the crusher pair of rolls has five adjustable parameters (λ, μ, γ, β, and ϕ) and each screen deck has three (a, m, and ρ). Before exploring the effect of the model parameters uncertainties on the optimal profiles, a sensitivity study was conducted in order to select the parameters that most influence the circuit dynamics. Consequently, different simulations were carried out starting from the proposed initial steady state (nominal plant capacity) and disturbing each parameter ±5% (percentage value based on the work performed by Wang and Cameron[16,35,36]). Considering that the PSD of the crusher outlet stream is mainly determined by the setting of the lower pair of rolls,[4] only the parameters corresponding to this pair of rolls were tested. Since both deck parameters are important in the screen classification, all of them were disturbed. The results from this sensitivity analysis indicated that the most influencing model parameters were μ of the lower pair of rolls and m of the bottom deck screen. Because the variables of the granulation circuit presented quite different steady-state deviations when both parameters were ±5% disturbed, the uncertainty level for μ and m was independently modified in order to obtain similar values for some key granulation circuit variables (the flow rate of the oversize stream fed to the crusher, and the PSDs mass arithmetic mean and standard deviation of the streams that leave the crusher and the bottom deck). From this analysis, disturbances of +3.5% and +20% for μ and m, respectively, were found as appropriate uncertainty levels.

Finally, the optimal control problems studied in the previous sections were run again considering in a first analysis a step change of +3.5% in μ and in a second one a step change of +20% in m. Both step changes were implemented 2 h after initializing the dynamic optimizations from the original steady-state (nominal plant capacity).

According to the outcomes presented in the previous section (base case, i.e. without taking into account model uncertainties) the optimal control problem with three manipulated variables (urea melt flow rate, granulator discharge area, and fluidization air flow rate) was the most attractive to increase plant capacity. Therefore, for this optimal control problem, the optimal trajectories of the manipulated variables were again established for +3.5% and +20% disturbances for μ and m parameters, respectively.

Figure 11 shows the effect of uncertainties in the bottom crusher parameter μ. It is demonstrated that the dynamic evolution of the percentage of discharge area for +3.5% μ and 0% μ are coincident. Regarding the urea melt and fluidization air flow rate transient profiles, the +3.5% μ case slightly differs from the base one. In fact, the dynamic deviations are lower than 0.4 and 0.75% for the melt and air flow rates, respectively. Furthermore, the optimized plant throughput remains almost constant (the plant capacity is just 1% higher than the one obtained using the model parameters corresponding to the base case).

On the other hand, Figure 12 presents the time trajectories of the three manipulated variables when the bottom deck m parameter is modified. Again, the percentage of discharge area for +20% m agrees with that of 0% m. Once more, the urea melt and fluidization air flow rate time profiles slightly differ from those obtained without disturbances in m (the deviations are lower than 3.3% for both variables). Therefore, the calculated optimal trajectories are quite similar to those corresponding to 0% m.

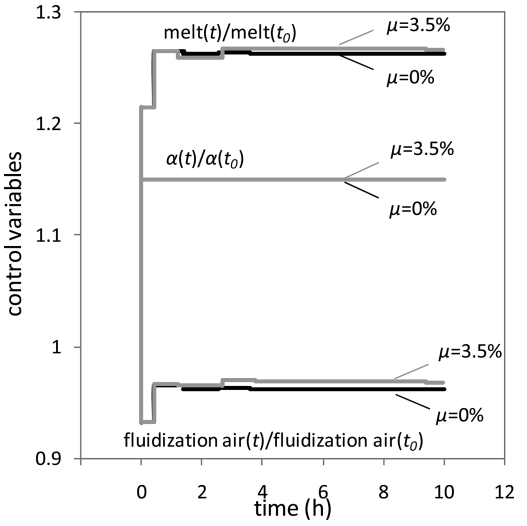

Figure 11. Control variables−time trajectories for three manipulated variables under a +3.5% μ disturbance.

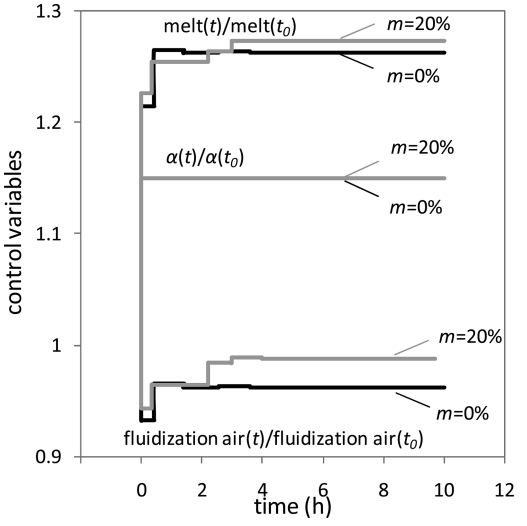

Figure 12. Control variables−time trajectories for three manipulated variables under a +20% m disturbance.

Overall, it can be concluded that the computed optimal profiles are not considerably sensitive to the assayed model uncertainties (which were selected based on a careful analysis of their influence on the circuit performance). Even though the results are not shown, the plant bottlenecks and their sequence of appearance are analogous to the ones identified for optimal problems assayed assuming the nominal model parameters (i.e., neglecting the parameters uncertainties).

4. CONCLUSIONS

The obtained results indicate that it is possible to increase plant production, without losing product quality and even decreasing the circuit recycle fraction, by selecting the appropriate manipulated variables and tracking their optimal time-trajectories. It is observed that the throughput increment is limited by the second growth chamber height in all the optimal control scenarios presented in this work. For the last two cases, before the maximum

allowable height is reached, the third chamber temperature and the product SGN constraints become active, respectively.

It is clearly demonstrated that the manipulation of just the granulator melt flow rate (trivial solution to the plant capacity revamping problem) does not improve the production in an attractive level because the physical constraints rapidly become active. The possibility of incorporating the granulator discharge area as a second control variable highly increases the urea product flow rate. The addition of the fluidization air flow rate and temperature as third and fourth control variables allow even higher increments in the throughput. Overall, the most significant bottlenecks—for the large-scale granulation plant under study—are the maximum allowable granulator discharge area and the minimum feasible fluidization air temperature. The results may encourage the replacement of discharge ducts by others with higher performance; however the discharge area size can be increased until the mass holdup within the chambers reaches the minimum allowable value. In that scenario, the temperatures within the growth chambers increase substantially, achieving the upper constraints. In this context, the addition of an efficient cooling air system to reduce the fluidization air inlet temperature becomes a good strategy for the whole circuit debottlenecking. Nevertheless, a cost analysis should be performed in order to determine if this strategy is economically worthwhile.

The encountered main bottlenecks are expected to be the same for large-scale plants based on similar granulation circuit technologies (i.e., fluidized bed and melt granulation, no fresh particles feed).

The optimization results obtained with the implemented circuit simulator show to be slightly sensitive to the uncertainties assayed in the model fitting parameters, for this reason the proposed optimal control policies are expected to be practically applicable.

As future work, there is a special interest in improving the dynamic optimizations by incorporating additional constraints regarding the range of operating conditions for which pure coating can be considered as the main size enlargement process.

APPENDIX

This appendix briefly presents the equations of the models corresponding to the circuit units described in Section 2.

Crusher Model. As reported by Cotabarren et al.,[4] the mass balance for the crushed product of size d_i was expressed as follows:

$$p_i = f_i(1-a_i) + (1-a'_i)\sum_{j=1}^{i-1} b_{i,j}\left[a'_j\left(\frac{p_j - f_j(1-a_j)}{(1-a'_j)}\right) + f_j a_j\right] \tag{A.1}$$

where f_i represents the fed mass of size d_i, a_i is the fraction selected for primary breakage, and a'_i is the probability of being selected for breaking again. $b_{i,j}$ is the mass of particles of size d_i generated by breakage of a fed d_j size. The $B_{i,j}$ function (i.e., the cumulative form of the $b_{i,j}$) was fitted by the following expression:

$$B_{i,j} = \begin{cases} 1 & 1 \le i \le j \\ \phi\left(\dfrac{d_{i-1}}{d_j}\right)^{\gamma} + (1-\phi)\left(\dfrac{d_{i-1}}{d_j}\right)^{\beta} & n \ge i > j \ge 1 \end{cases} \tag{A.2}$$

Besides, a_i was expressed as

$$a_i = \frac{1}{1 + \left(\dfrac{d_i}{\dfrac{d_g}{\mu}}\right)^{-\lambda}} \tag{A.3}$$

The a'_i values were empirically related to the a_i ones as follows:

$$a'_i = \begin{cases} a_{i-1} & i < i_g - 1 \\ \dfrac{a_{i_g-1} + a_{i_g-2}}{2} & i = i_g - 1 \\ a_i & i \ge i_g \end{cases} \tag{A.4}$$

with d_g being the gap size and i_g being the size interval number corresponding to d_g.

For a given feed size distribution and a set gap, eq A.1 was solved together with the expressions A.2, A.3, and A.4 to predict the particle size distribution of the crusher product, prior estimation of the parameters λ, μ, γ, β, and ϕ. The values for these parameters were fitted by Cotabarren et al.[4] to properly describe available crusher data from a large-scale urea granulation plant.

Screen Model. Cotabarren et al.[20] reported the mathematical model to properly represent the operation of double deck screens for urea granules size classification. To represent a non-ideal classification operation, oversize partition coefficients for each size class were used. For each size class i, the oversize partition coefficient (T_i) is defined as the amount of oversize within class i divided by the amount of material of that size in the feed.

$$T_i = \frac{F_O X_{Oi}}{F X_{Fi}} \tag{A.5}$$

The undersize stream for the solids belonging to each size class i was calculated through simple mass balances.

$$F_U X_{Ui} = (1 - T_i) F X_{Fi} \tag{A.6}$$

Several models are proposed for the partition coefficients, Cotabarren et al.[20] used the following expression:

$$T_i = 1 - \exp\left(-0.693\left(\frac{d_i}{d_{50}}\right)^m\right) \tag{A.7}$$

where d_{50} is the particle size distribution (PSD) cut size. The following d_{50} correlation was chosen by Cotabarren et al.:[20]

$$d_{50} = h\left(\frac{\dfrac{U^T}{S}}{K}\right)^a \tag{A.8}$$

where h is the screen aperture and U_T is the theoretical undersize mass flow fed to the screen, S is the screen surface, K is a product of factors that correct the screen basic capacity, and a is a fitting parameter.

The variable K is given by

$$K = ABCDEF_D G \tag{A.9}$$

The expressions for these parameters can be found elsewhere.[20]

The model involves three parameters to be adjusted: a, the Plitt's parameter m, and the bulk density (ρ) of the material on the deck required to calculate F_D. Cotabarren et al.[20] fitted all the

adjustable parameters using available experimental data collected from a high-capacity urea plant.

Granulator and Fluidized Bed Cooler Model. In this work, the granulator model (constituted by six chambers, $k = 6$) developed by Bertin et al.[21] was implemented. The dynamic urea mass balance for a chamber k was given by the authors as[21]

$$\frac{dm_T^k}{dt} = \dot{m}_{in}^k + \dot{m}_{melt}^k(1 - x_{melt}^k) - \dot{m}_{out}^k \quad m_T^k(0) = m_{T0}^k \tag{A.10}$$

where t represents the time, m_T^k, $\dot{m}_{in}^k$, and $\dot{m}_{out}^k$ are the solid mass holdup, inlet and outlet particles mass flow rates, respectively. $\dot{m}_{melt}^k$ and x_{melt}^k are the urea solution mass flow rate atomized into chamber k and its water mass fraction, respectively. The outlet solids mass flow rates were obtained by applying the Bernoulli equation

$$\dot{m}_{out}^k = C_D A_o^k \sqrt{2g\rho_{bed}^k(\rho_{bed}^k H_k - \rho_{bed}^{k+1} H_{k+1})} \quad k = 1 \text{ to } 5 \tag{A.11}$$

$$\dot{m}_{out}^6 = C_D A_o^6 \rho_{bed}^6 \sqrt{2gH_6} \tag{A.12}$$

where A_0^k and H_k are the passage area and fluidized bed height of chamber k, respectively. C_D is the discharge coefficient and ρ_{bed}^k is the bed density.

To complete the set of equations, the fluidized bed height within each chamber was computed as

$$H_k = \frac{m_T^k}{\rho_{bed}^k A_T^k} \tag{A.13}$$

with A_T^k being the cross-sectional area of chamber k.

The following dynamic energy balance given by Bertin et al.[21] was considered to compute the temperature T_k in each chamber.

$$\begin{aligned} m_T^k Cp_u(T_k)\frac{dT_k}{dt} &= \dot{m}_{in}^k \int_{T_{k-1}}^{T_k} Cp_u dT \\ &+ \dot{m}_{melt}^k(1 - x_{melt}^k) \int_{T_{melt}^k}^{T_k} Cp_u dT \\ &+ \dot{m}_{melt}^k x_{melt}^k \int_{T_{melt}^k}^{T_k} Cp_w dT - \dot{m}_{melt}^k x_{melt}^k \Delta H_{EV}(T_k) \\ &+ \dot{m}_{melt}^k(1 - x_{melt}^k)\Delta H_{DIS}(T_{melt}^k) \\ &+ \dot{m}_a^k \int_{T_a^k}^{T_k} Cp_a dT + \dot{m}_a^k Y^k \int_{T_a^k}^{T_k} Cp_v dT \quad T_k(0) = T_0^k \end{aligned} \tag{A.14}$$

where T_{melt}^k, T_a^k, and T_{k-1} are the temperatures of the melt, fluidization air, and solids entering to chamber k, respectively. T_k is the chamber temperature and according to previous studies[3] can be accurately considered equal to the outlet solid and air temperatures. ΔH_{DIS} and ΔH_{EV} are the latent heats associated to the urea melt dissolution and water evaporation. Cp_u, Cp_w, Cp_a and Cp_v are the mass heat capacities of the solid urea, liquid water, air and water vapor, respectively.

The growth chambers' mass A.10 and the energy A.14 balances were adapted to represent the cooling compartments (k from 3 to 6) by setting the urea mass flow rate equal to zero.

Bertin et al.[21] developed a population balance model for the urea fluidized bed granulator assuming that only growth by coating occurs (elutriation, agglomeration, breakage, attrition, and nucleation were supposed negligible). Therefore, the dynamic PBE for each well-mixed granulation chamber was given by

$$\frac{\partial n^k}{\partial t} + \frac{\partial(G_k n^k)}{\partial d} = \dot{n}_{in}^k - \dot{n}_{out}^k \tag{A.15}$$

with G_k being the growth rate, d being the particle diameter, and $\dot{n}_{in}^k$ and $\dot{n}_{out}^k$ the number density function flows in and out of the chamber k, respectively. The PBE discretization technique developed by Hounslow and Marshall[34] and adopted by Bertin et al.[21] was implemented to solve the discretized form of eq A.15 together with the initial condition $n^k(d,0) = n_0^k$.

Assuming that particles belonging to different size intervals grow proportional to its fractional surface area, G_k was defined as[21]

$$G_k = \frac{2\dot{m}_{melt}^k(1 - x_{melt}^k)}{\rho_p A p_T^k} \tag{A.16}$$

where Ap_T^k denotes the total particle superficial area within chamber k, and ρ_p represents the particle density. This equation states that all the particles, independently of their sizes, grow at the same rate.[21,32,33]

The fluidized bed cooler was represented as a continuous stirred tank analogous to one granulator cooling chamber, i.e., assuming that $\dot{m}_{melt} = 0$.[22]

AUTHOR INFORMATION

Corresponding Author

*Tel.: 54-291-486-1700, ext. 269. Fax: 54-291-486-1600. E-mail: icotabarren@plapiqui.edu.ar.

ACKNOWLEDGMENT

We express our gratitude for financial support by the Consejo de Investigaciones Científicas y Técnicas (CONICET), Agencia Nacional de Promoción Científica y Tecnológica (ANPCyT), and Universidad Nacional del Sur (UNS) of Argentina.

NOTATION

A = Screen basic capacity (kg/s m^2)
A_0^k = Granulator passage area between chambers, for chamber k (m^2)
A_T^k = Granulator cross sectional area, for chamber k (m^2)
a = Screen fitting parameter (-)
a_i = Probability of a particle from size d_i to undergo primary breakage (-)
a'_i = Probability of a particle from size d_i to rebreak (-)
Ap_T^k = Total particle superficial area within chamber k (m^2)
B = Factor for % of oversize in the screen feed (-)
$b_{i,j}$ = Breakage function, mass fraction of particles of size d_i generated by breakage of d_j size particles (-)
$B_{i,j}$ = Cumulative breakage function, mass fraction of particles smaller than size d_i generated by breakage of d_j size particles (-)
C = Factor for % of half-size under in the screen feed (-)
C_D = Granulator solids discharge coefficient (-)
Cp_a = Air mass heat capacity (J/kg K)
Cp_u = Solid urea mass heat capacity (J/kg K)
Cp_v = Water vapor mass heat capacity (J/kg K)
Cp_w = Liquid water mass heat capacity (J/kg K)
D = Factor for deck location (-)

d = Particle diameter (m)
d_i = Particle size (mm)
d_j = Particle size (mm)
d_g = Gap size (mm)
d_{50} = Screen cut size (mm)
d_{50} BD = Bottom deck screen cut size (mm)
d_{50} TD = Top deck screen cut size (mm)
E = Factor for wet screening (-)
F = Screen feed mass flow rate (kg/s)
F_D = Screen bulk density factor (-)
f_i = Crusher feed mass percent of size d_i (%)
F_O = Screen oversize mass flow rate (kg/s)
FO = Value of the objective function (-)
F_P = Screen product mass flow rate (kg/s)
F_U = Screen undersize mass flow rate (kg/s)
g = Gravity acceleration (m/s^2)
G = Factor for % near-size in the screen feed (-)
G_k = Growth rate, for chamber k (m/s)
h = Screen aperture (mm)
h_k = Height of chamber k = H_k /H_{weir}, k = 1 to 6 (-)
H_k = Height of chamber k, k = 1 to 6 (m)
H_{weir} = Weir height (m)
i = Size class index (-)
i_g = Number of size interval corresponding to d_g (-)
j = Size class index (-)
k = Chamber number (-)
K = Screen correction parameter
m = Plitt's adjustable parameter (-)
$\dot{m}_a^k$ = Fluidization air mass flow rate for granulator chamber k, dry basis (kg/s)
$\dot{m}_{in}^k$ = Particle mass flow rate entering granulator chamber k (kg/s)
$\dot{m}_{melt}^k$ = Urea melt mass flow rate to granulator chamber k (kg/s)
$\dot{m}_{out}^k$ = Particle mass flow rate coming out of granulator chamber k (kg/s)
m_T^k = Solids mass holdup in granulator chamber k (kg)
n^k = Number density function in chamber k (no./m)
$\dot{m}_{in}^k$ = Number density function flowing in chamber k (no./m s)
$\dot{m}_{out}^k$ = Number density function flowing out of chamber k (no./m s)
PBE = Population Balance Equation (-)
p_i = Crusher product mass percent of size d_i (%)
PSD = Particle Size Distribution
R = Recycle fraction (-)
S = Screen surface (m^2)
SGN = Size Guide Number, particle size corresponding to the 50% of the mass cumulative size distribution (mm × 100)
$SGN_{product}$ = Size Guide Number corresponding to the product stream (mm × 100)
t = Time (s)
t_0 = Initial simulation time (s)
Ta_2 = Second chamber fluidization air temperature (K)
T_a^k = Fluidization air temperature for chamber k (K)
t_f = Final simulation time (s)
T_i = Oversize partition coefficient for each size interval i (-)
T_k = Temperature in chamber k, k = 1 to 6 (K)
T_{melt}^k = Urea melt temperature for chamber k (K)
U^T = Theoretical undersize mass flow fed to the screen, (kg/s)
$u(t)$ = Control variables (-)
$W_{2-4\ mm}$ = Mass fraction of product within the size range 2 − 4 mm (-)
w = Constraints value (-)
w^{max} = Constraints upper limit (-)
w^{min} = Constraints lower limit (-)
x_{melt}^k = Fraction of water in the melt stream of chamber k (-)
$x(t)$ = State variables of the process model (-)
X_{Fi} = Mass fraction of each size interval in feed to screen (-)
X_{Oi} = Mass fraction of each size interval in oversize from screen (-)
X_{Ui} = Mass fraction of each size interval in undersize from screen (-)
Y^k = Mass air humidity in chamber k, dry basis ($kg_{water}/kg_{dry\ air}$)
z = Violation variable for path constraints formulation (-)

GREEK SYMBOLS

α	Fraction of discharge area (-)
β	Adjustable parameter corresponding to the B_{ij} function (-)
γ	Adjustable parameter corresponding to the B_{ij} function (-)
ΔH_{DIS}	Latent heat capacity of urea melt dissolution (J/kg)
ΔH_{EV}	Latent heat capacity of water evaporation (J/kg)
ε	Minimum tolerance for path constraints violation (-)
λ	Adjustable parameter corresponding to the a_i function (-)
μ	Adjustable parameter corresponding to the a_i function (-)
ρ	Adjustable parameter corresponding to the F_D factor (kg/m^3)
ρ_{bed}^k	Fluidized bed density for chamber k (kg/m^3)
ρ_p	Particle density (kg/m^3)
τ_k	Particle residence time in chamber k (s)
ϕ	Adjustable parameter corresponding to the B_{ij} function (-)

REFERENCES

(1) Balliu, N. E.; Cameron, I. T. Performance Assessment and Model Validation for an Industrial Granulation System. *Powder Technol.* **2007**, *179*, 12–24.

(2) Heffer, P.; Prud'homme, M. Fertilizer Outlook 2010−2014. *78th IFA Annual Conference*, Paris, France, May 2010.

(3) Bertín, D. E.; Mazza, G. D.; Piña, J.; Bucalá, V. Modeling of an Industrial Fluidized Bed Granulator for Urea Production. *Ind. Eng. Chem. Res.* **2007**, *46*, 7667–7676.

(4) Cotabarren, I.; Schulz, P. G.; Bucalá, V.; Piña, J. Modeling of an Industrial Double Roll Crusher of a Urea Granulation Circuit. *Powder Technol.* **2008**, *183* (2), 224–230.

(5) Heinrich, S.; Peglow, M.; Mörl, L. Particle Population Modeling in Fluidized Bed Spray Granulation - Analysis of the Steady State and Unsteady Behaviour. *Powder Technol.* **2003**, *130*, 154–161.

(6) Adetayo, A. A.; Litster, J. D.; Cameron, I. T. Steady State Modeling and Simulation of a Fertilizer Granulation Circuit. *Comput. Chem. Eng.* **1995**, *19*, 383–393.

(7) Wildeboer, W. J. *Steady State and Dynamic Simulations of a Closed Loop Granulation Circuit.* Master Thesis, Delft University of Technology, The Netherlands, 1998.

(8) Adetayo, A. A. *Modelling and Simulation of the Fertilizer Granulation Circuit.* PhD Thesis, University of Queensland Australia, 1993.

(9) Balliu, N. E. *An Object Oriented Approach to the Modeling and Dynamics of Granulation Circuits.* PhD. Thesis, University of Queensland, Australia, 2005.

(10) Zhang, J.; Litster, J. D.; Wang, F. Y.; Cameron, I. T. Evaluation of Control Strategies for Fertilizer Granulation Circuits Using Dynamic Simulation. *Powder Technol.* **2000**, *108*, 122–129.

(11) Potmann, M.; Ogunnaike, B. A.; Adetayo, A. A. Model-based Control of a Granulation Circuit. *Powder Technol.* **2000**, *108*, 192–201.

(12) Gatzke, E. P.; Doyle, F. J., III Model Predictive Control of a Granulation Circuit Using Soft Output Constraints and Prioritized Control Objectives. *Powder Technol.* **2001**, *121*, 149–158.

(13) Sanders, C. F. W.; Hounslow, M. J.; Doyle, F. J., III Identification of Models for Control of Wet Granulation. *Powder Technol.* **2009**, *188* (3), 255–263.

(14) Glaser, T.; Sanders, C. F. W.; Wang, F. Y.; Cameron, I. T.; Litster, J. D.; Poon, J. M. H.; Ramachandran, R.; Immanuel, C. D.; Doyle, F. J., III *J. Process Control* **2009**, *19*, 615–622.

(15) Wang, F. Y.; Ge, X. Y.; Balliu, N.; Cameron, I. T. Optimal Control and Operation of Drum Granulation Processes. *Chem. Eng. Sci.* **2006**, *61* (1), 257–267.

(16) Wang, F. Y.; Cameron, I.T. A Multi-form Modelling Approach to the Dynamics and Control of Drum Granulation Processes. *Powder Technol.* **2007**, *179* (1−2), 2–11.

(17) Heinrich, S.; Peglow, M.; Ihlow, M.; Henneberg, M.; Mörl, L. Analysis of the Start-up Process in Continuous Fluidized Bed Spray Granulation by Population Balance Modelling. *Chem. Eng. Sci.* **2002**, *27*, 4369–4390.

(18) Drechsler, J.; Peglow, M.; Heinrich, S.; Ihlow, M.; Mörl, L. Investigating the Dynamic Behavior of Fluidized Bed Spray Granulation Processes Applying Numerical Simulation Tools. *Chem. Eng. Sci.* **2005**, *60*, 3817–3833.

(19) Radichkov, R.; Müller, T.; Kienle, A.; Heinrich, S.; Peglow, M.; Mörl, L. A Numerical Bifurcation Analysis of Continuous Fluidized Bed Spray Granulation with External Product Classification. *Chem. Eng. Process.* **2006**, *45*, 823–837.

(20) Cotabarren, I. M.; Rossit, J.; Bucalá, V.; Piña, J. Modeling of an Industrial Vibrating Double-Deck Screen of a Urea Granulation Circuit. *Ind. Eng. Chem. Res.* **2009**, *48* (6), 3187–3196.

(21) Bertín, D.; Cotabarren, I.; Bucalá, V.; Piña, J. Analysis of the Product Granulometry, Temperature and Mass Flow of an Industrial Multichamber Fluidized Bed Urea Granulator. *Powder Technol.* **2010**, *206*, 122–131.

(22) Cotabarren, I. M.; Bertín, D.; Romagnoli, J.; Bucalá, V.; Piña, J. Dynamic Simulation and Optimization of a Urea Granulation Circuit. *Ind. Eng. Chem. Res.* **2010**, *49* (14), 6630–6640.

(23) Kayaert, A. F.; Antonus, R. A. C. Process for the Production of Urea Granules, US Patent 5 (653), 1997, 781.

(24) CF Industries. Deerfield, Illinois, USA; http://www.cfindustries.com/ProductUrea.htm.

(25) Karnaphuli Fertilizer Company Limited. Rangadia, Anowara Chittagong, Bangladesh; http://www.kafcobd.com/html/products.html.

(26) gPROMS Documentation, Release 3.2.0; Process Systems Enterprise Ltd.: London, United Kingdom, 2009.

(27) Kiss, A. A.; Bildea, C. S.; Grievink, J. Dynamic Modelling and Process Optimization of an Industrial Sulfuric Acid Plant. *Chem. Eng. J.* **2010**, *158*, 241–249.

(28) Lopez, J. A.; Bucalá, V.; Villar, M. Application of Dynamic Optimization Techniques for Poly(β-hydroxybutyrate) Production in a Fed-Batch Bioreactor. *Ind. Eng. Chem. Res.* **2010**, *49*, 1762–1769.

(29) Tzolakis, G.; Papanikolau, P.; Kolokotronis, D.; Samaras, N.; Tourlidakis, A.; Tomboulides, A. Emissions' Reduction of Consumption Through Simulation and Optimization of its Mathematical Model. *Oper. Res. Int. J.* **2010**, *10*, 71–89.

(30) Asteasuain, M.; Bandoni, A.; Sarmoria, C.; Brandolin, A. Simultaneous Process and Control System Design for Grade Transition in Styrene Polymerization. *Chem. Eng. Sci.* **2006**, *61*, 3362–3378.

(31) Nowee, S. M.; Abbas, A.; Romagnoli, J. A. Model-Based Optimal Strategies for Controlling Particle Size in Antisolvent Crystallization Operations. *Cryst. Growth Des.* **2008**, *8* (8), 2698–2706.

(32) Litster, J.; Ennis, B.; Liu, L. *The Science and Engineering of Granulation Processes*; Particle Technology Series; Kluwer Academic Publishers: Dordrecht, 2004.

(33) Mörl, L.; Heinrich, S.; Peglow, M. Fluidized Bed Spray Granulation. In Salman, A. D., Hounslow, M. J., Seville, J. P. K., Eds.; *Handbook of Powder Technology*; Elsevier: Amsterdam, 2007.

(34) Hounslow, M. J.; Ryall, R. L.; Marshall, V. R. A Discretized Population Balance for Nucleation, Growth, and Aggregation. *AIChE J.* **1988**, *34* (11), 1821–1832.

(35) Cameron, I. T.; Wang, F. Y. Process System Engineering Applied to Granulation. In Salman, A. D., Hounslow, M. J., Seville, J. P. K., Eds.; *Handbook of Powder Technology*; Elsevier: Amsterdam, 2007.

(36) Wang, F. Y.; Cameron, I. T. In *7th World Congress of Chemical Engineering*; Glasgow, Scotland, 2007.